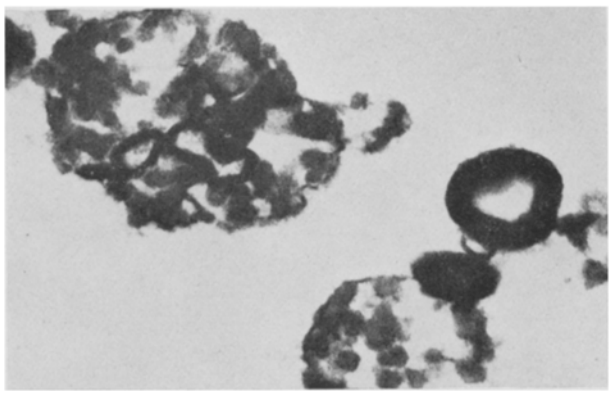

Fig. 3. Protamine induced configurational changes in 'crystal-like' structures. Protamine was added into the boiled mitochondria (exp. 3). ×34,000.

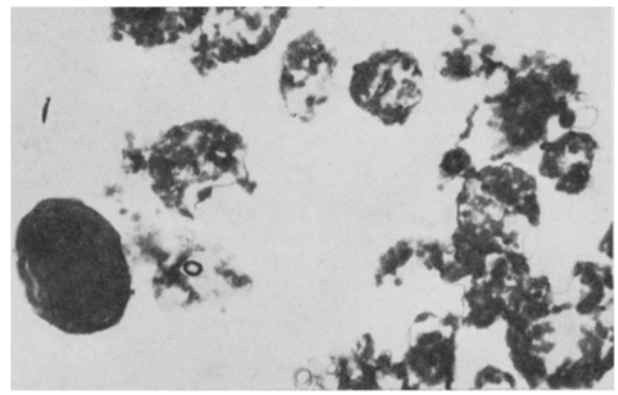

Fig. 4. Experiment 4 as in experiment 3. ×15,500.

The possibility that this 'membrane derived' paracrystalline material can play a role in ultrastructural transtions in mitochondria was examined electron microscopically by observations of interaction between 'crystal-like' structures and protamine.

As is shown in Figure 2, protamine prevented formation of 'crystal-like' structures when added to the mitochondrial suspension before boiling. Protamine added into the heated mitochondria induced ultrastructural transitions in paracrystalline structures already formed (Figure 3 and 4). In all experiments with protamine, occurence of typical 'myelin figures' can be detected, instead of typical for heated mitochondria 'crystal-like' structures. It is interesting that similar changes occured when protamine was repleaced by cytochrome c (not shown).

The direction of ultrastructural transitions observed is the same as that reported in intact mitochondria upon addition of protamine, visualized as a strong contraction of all membranous material in mitochondria[4–6]. It is possible that the substance interacting with protamine in intact mitochondria is the same as is visualized as a paracrystalline material after boiling. Observations that upon addition of protamine this 'membrane derived' paracrystalline material could form 'myelin structures', suggest that protamine is incorporated into paracrystalline material. This binding is probably related to the presence of lipids. This suggestion is in accordance with observations of RAND and SENGUPTA[16] of formation of lattice structures by cardiolipin, and is confirmed by our observations that similar paracrystalline structures as observed in boiled mitochondria were visualized in intact, unboiled beef heat mitochondria incubated with cardiolipin[2,3].

Binding of protamine into structural elements of membrane of intact mitochondria would change the value of proton motive force (PMF) as well as a ratio of $\Delta\Psi/\Delta$pH in PMF, leading to the inhibition of respiration. This inhibition we found to be reversed by energy 'releasing systems': ATP synthesis or action of uncouplers[17,18].

Résumé. La protamine provient de structures paracrystallines, résultant de la décomposition thermique des membranes mitochondriennes. Après la formation de ces structures, l'addition de la protamine les rend miéliniques.

J. POPINIGIS and TERESA WRZOŁKOWA

Department of Biochemistry;
Laboratory of Electron Microscopy, Medical School,
Al. Zwycięstwa 42, Gdańsk 6 (Poland),
24 April 1972.

[16] R. P. RAND and S. SENGUPTA, Biochim. biophys. Acta *255*, 484 (1972).
[17] J. POPINIGIS, W. RZECZYCKI and J. SWIERCZYNSKI, FEBS Lett. *8*, 149 (1970).
[18] J. POPINIGIS, J. M. SMOLY, R. F. BRUCKER and C. H. WILLIAMS, Proc. of 8th FEBS Meeting (Elsevier, Amsterdam 1972), Abstr. 634.

On the Ultrastructure of Mammalian Tendon

The collagen fibers which are the major structural component of rat tail tendon (RTT) have been noted for some time to follow some wavy course through the tendon bundle, and become straight and parallel to the tendon axis only when the tendon is stretched[1]. Different workers, using different techniques, have characterized the waveform variously as planar or helical, either with or without intertwining of the fibers. Recently, DIAMANT, KELLER et al.[2] analyzed the shape of the waveform in RTT in considerable detail by the straightforward technique of polarizing microscopy, and demonstrated that it is a planar wave shape. When the tendon was teased down to fine bundles, it was observed that the physical outlines of these sub-bundles followed the waveform as that deduced from the polarizing optics of the intact tendon bundle. They also observed that straightening of the waveform, rather than extension of the collagen fibers themselves, is the principal mechanism of deformations in the range expected in vivo, and deduced that the independent me-

[1] D. H. ELLIOTT, Biol. Rev. *40*, 392 (1965).
[2] J. DIAMANT, A. KELLER, E. BAER, M. LITT and R. G. C. ARRIDGE, Proc. R. Soc. B *180*, 293 (1972).

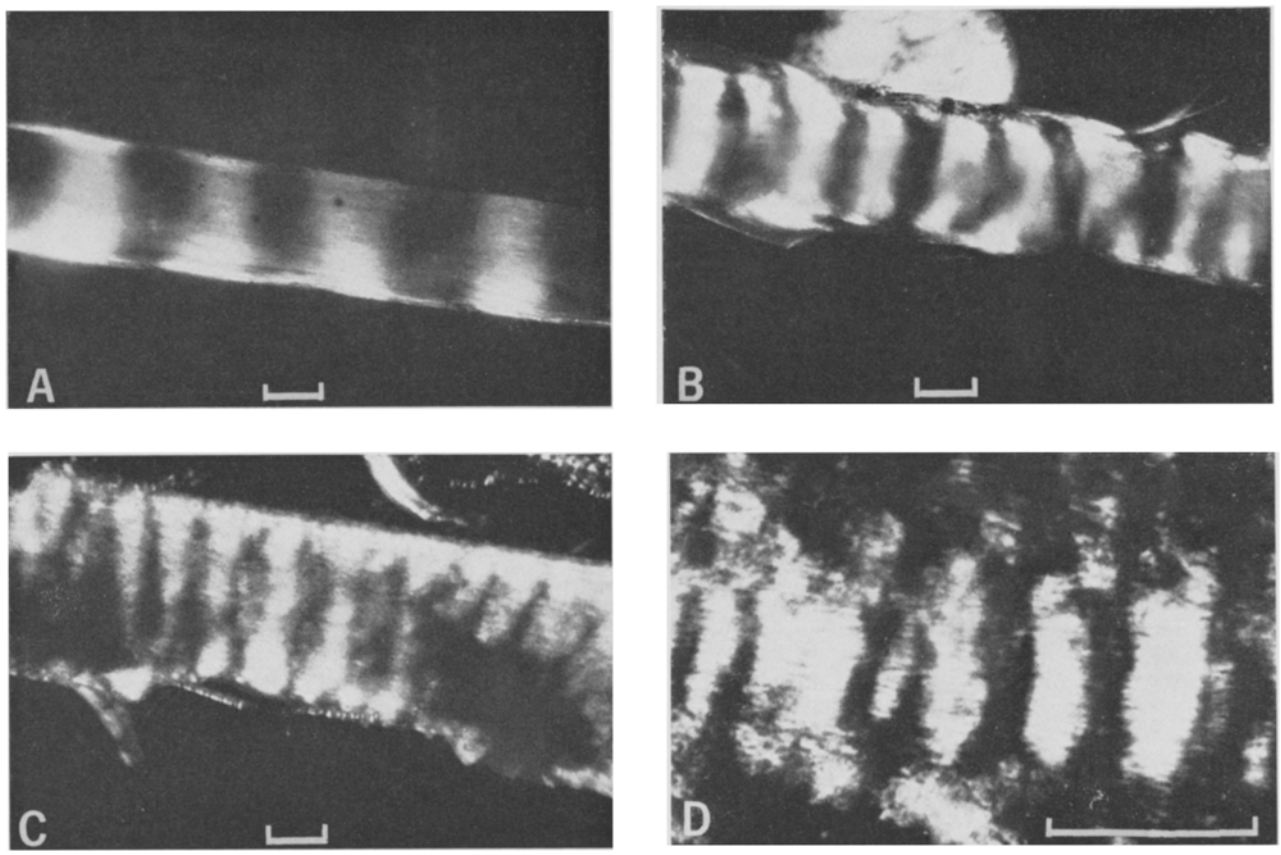

Fig. 1. Micrographs in transmitted polarized light of: a) rat tail tendon, 14-month-old; b) kangaroo tail tendon, 12 years old; c) human central diaphragm tendon, 51 years old; and d) human Achilles tendon, 46 years old. Scale bar is 100 microns.

Typical wave parameters from various tendons

Source and age	l_o [microns]	Θ_o [degrees]
Rat tail (14 months)	100	12
Human diaphragm (51 years)	60	12
Kangaroo tail (11.7 years)	75	8–9
Human achilles (46 years)	20–50	6–8

Definition of wave parameters

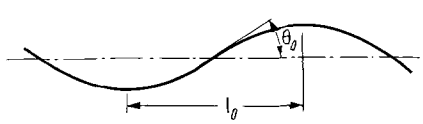

chanical element is a collagen fiber whose diameter increases from 1000 to 5000 Å as the rat aged. This is essentially the same size as the collagen fibers frequently observed by electron microscopy.

The purpose of this note is to show that the planar waveform and its effects on mechanical properties are not peculiar to RTT, but also apply to other mammalian tendon which differs from RTT firstly by being subjected to far greater load and impact requirements over a much longer lifespan of the organism, and secondly by being much more difficult to obtain as experimentally tractable fiber bundles. Figure 1 shows polarizing micrographs of samples from rat tail, kangaroo tail, human central diaphragm, and human Achilles tendons. In each case the waveform is seen as alternating light and dark bands across the fiber bundle. Reference 2 develops in detail the techniques and reasoning by which the shape and size parameters of the waveform can be deduced from the presence of these bands and their behavior as the bundle axis is rotated with respect to the polarizers, and as the bundle is rotated about its own axis. In Figure 1, the axis of each fiber bundle is rotated with respect to the polarizer by the angle, Θ_o, which produced optimum contrast between transmitting and extinguishing regions of the sample. Rotating the sample to the corresponding negative angle, $-\Theta_o$, produced a similar banding, but the regions which transmitted at $+\Theta_o$ extinguised at $-\Theta_o$ and conversely, showing that the waveform is symmetric. The fiber bundles of the human tendons are difficult to remove from the tough surrounding substance, and we have not yet been successful in removing samples which are suitable for rotation about the tendon axis. Such rotation of the kangaroo tail tendon, however, showed a position of optimum contrast (shown in Figure 1), and positions of minimum or no contrast at $\pm$ 90° additional rotation, demonstrating that the waveform here is also planar.

As the tendons were stretched, the waveform was straightened out. We observed that the angle at which the contrast was optimum decreased from Θ_o to some lesser value, α, and became zero at sufficiently large strain, although measurement of small angles was quite difficult. The relation between the angle of the waveform and the strain of the tendon was developed for inextensible fibers of 4 possible wave shapes: a helix, a planar sine wave, a planar

zig-zag with hingend apices which deforms by unfolding, and a planar zig-zag with rigid apices which deforms by cantilever bending (the last is derived in ref.[2]). In Figure 2, the data for 2 types of tendon are compared to the predicted curves, and it is seen that the points lie along the curve for the sine wave, or between the sine and cantibending cases. It is also noted that the human diaphragm tendon data lie in the same relation to the predicted curves as do the RTT data, where the waveform can be demonstrated planar by rotation in polarized light. This strongly indicates that the waveform is also planar in the diaphragm tendon.

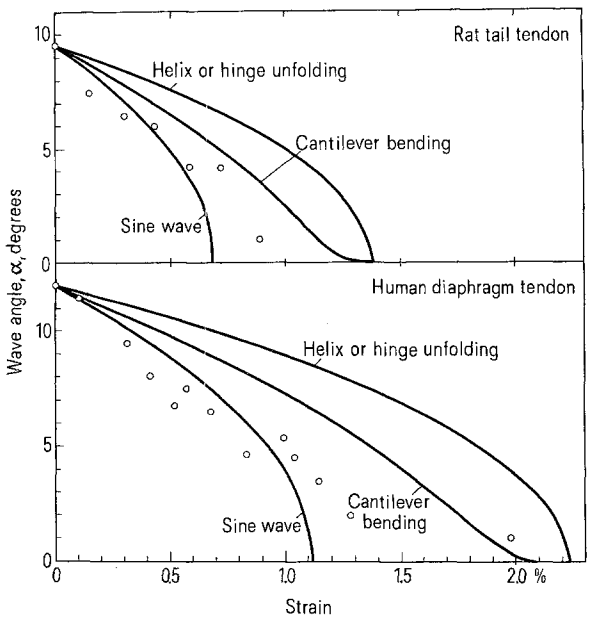

Fig. 2. Decrease of angle of the waveform with strain as tendon is stretched, for rat tail and human diaphragm tendons. (Samples A) and C) in Figure 1). Points are experimental observations and curves are predicted behavior of inextensible fibers whose original wave shape is as marked.

The Table shows that major differences were found in the size parameters of the waveform for tendons from different sources. Also, a range of sizes was found in individual samples of human Achilles and kangaroo tail tendon, including a waveform 100 μm long in the Achilles tendon of an 87-year-old male. Nonetheless, it seems clear that essentially the same planar symmetric waveform as seem in RTT was found in all these tendons from diverse sources. Consequently, its implications for the stress response and function of the tendon in vivo, along the lines of ref.[2], are expected to hold throughout[3].

Zusammenfassung. Es wird gezeigt, dass die zwischen gekreuzten Nicols für die Rattenschwanzsehne nachgewiesenen periodischen Bänder von fibrillären Strukturelementen ebener Wellenform abstammen und deren Ausstreckung das beobachtete Dehnungsverhalten erklärt[2], das auch für andere Säugetiere zutrifft.

W. C. Dale[4], E. Baer[4], A. Keller[5] and R. R. Kohn[6]

Division of Macromolecular Science, Case Western Reserve University, Cleveland (Ohio 44106, USA); H. H. Wills Physics Laboratory, University of Bristol, Tyndall Avenue, Bristol, BS81TL (England); and Institute of Pathology, Case Western Reserve University (USA), 23 March 1972.

[3] Support of the U.S. National Institutes of Health, under grant No. T01 HD00304-01, is gratefully acknowledged.

[4] Division of Macromolecular Science, Case Western Reserve University, Cleveland (Ohio 44106, USA).

[5] H. H. Wills Physics Laboratory, University of Bristol, Tyndall Avenue, Bristol, BS 81 TL England).

[6] Institute of Pathology, Case Western Reserve University (USA).

Chemical and Immunological Characterization of Serum Lipoproteins Isolated by Glass-Column Chromatography

The chromatographic separation of lipoproteins by adsorption on glass powder columns, developed for whole serum by Carlson[1], was adopted with some modifications for isolation of serum lipoproteins from human, rabbit and rat subjects. Assay of the column eluates by both chemical and immunoreaction methods demonstrated the reliability of this method for a satisfactory separation.

Experimental. Stock solutions of 1.2 *M* potassium bicarbonate and 0.4 *M* potassium carbonate were prepared and titrated against HCl. Buffer solutions of pH 8.8, pH 9.6 and pH 9.8 were prepared from stock solutions. Glass columns, 15 × 150 mm, were packed with glass-beads of 100–150 mesh and serum samples, diluted with equal volume of buffer pH 8.8, were added to the columns. The walls were washed with 1 ml of pH 8.8 buffer. The samples were allowed to move down the columns by opening the stopcock. The columns were washed with another portion of pH 8.8 buffer in the order: 2 + 2 + 4 + 4 ml, followed by 1 ml of 15 ml of the pH 8.8 eluate, containing mainly albumin, were collected. The subsequent fractions of the buffer eluates were collected in the following order: 5 ml + 5 ml + 3 ml of pH 9.6 and 2 ml of 9.8 were collected together as containing α-lipoprotein. Then 5 ml of 0.4 *M* potassium carbonate buffer were collected as α_2 lipoprotein. Finally 15 ml of potassium carbonate buffer were added to the column for elution of β-lipoprotein.

The lipoprotein fractions obtained after elution from the glass-columns were dialyzed against distilled water for 8 h at 4 °C. The solutions were lyophilized and stored for 6 weeks at −15 °C without any appreciable denaturation. The ultra-centrifugal pattern of the separated α- and β-lipoproteins in artificial boundary cells with Schilieren optics are shown (Figures 1 and 2).

The protein fractions of the lipoproteins and sera were determined according to Lowry et al[2]. Total and free cholesterol were estimated by the method of Sperry and

[1] L. A. Carlson, Clin. chim. Acta *5*, 528 (1960).

[2] O. H. Lowry, N. J. Rosebrough, A. L. Farr and R. L. Randall J. biol. Chem. *193*, 265 (1951).